Chemical and Electronic Branching Ratios in the Chemiluminescent Reactions of Hyperthermal Ca(^{3}P) Atoms with CF_2Cl_2 and $CF_2{=}CCl_2$

Gustavo A. Pino, Carlos A. Rinaldi, and Juan C. Ferrero*

INFIQC, Departamento de Físico Química, Facultad de Ciencias Químicas, Universidad Nacional de Córdoba, Ciudad Universitaria, (5000) Córdoba, Argentina

Received: September 6, 2002; In Final Form: June 12, 2003

Chemiluminescent reactions of hyperthermal Ca(^{3}P) with CF_2Cl_2 and $CF_2{=}CCl_2$ were studied in a beam-gas arrangement under single collision conditions. Emissions associated with the $A(^2\Pi_\Omega) \rightarrow X(^2\Sigma^+)$ and the $B(^2\Sigma^+) \rightarrow X(^2\Sigma^+)$ transitions from CaCl and CaF were observed for both reactions. The chemical and electronic branching ratios were determined for these reactions, and different results were obtained for each one. The different behavior was rationalized by a simple MO pictures. For the case of the reaction with CF_2Cl_2 it was assumed that an electron from Ca(^{3}P) is transferred to a σ^*(C−Cl) orbital in CF_2Cl_2 which, at higher translational energies can also enter into a σ^*(C−F) orbital of the same molecule. In both cases the molecular anion produced is short-lived and will undergo fast decay to Cl^- or F^- to yield CaCl and CaF. For the reaction with $CF_2{=}CCl_2$ the electron from Ca(^{3}P) is transferred to a π^* orbital of the reagent molecule that generates a relatively stable molecular anion with $^2\Pi$ symmetry. This anion subsequently cross over several repulsive $^2\Sigma$ surfaces associated with σ^* orbitals of the C−Cl and the C−F bonds, to dissociate into Cl^- or F^- to produce CaCl and CaF. The electronic branching ratios are in good agreement with statistical distribution based on information theory approach, assuming the rigid rotor harmonic oscillator (RROH) approximation for the reaction with CF_2Cl_2 and the formation of a collision complex for the reaction with $CF_2{=}CCl_2$.

1. Introduction

The study of chemical reactions with electronically excited atoms constitutes one of the most active fields of research in reaction dynamics. In these reactions, measurement of the product chemiluminescence has provided to be one of the best methods to obtain information on the internal energy distribution and electronic populations in the reaction products.[1−13] This technique has been extensively used to study the reactions of alkaline-earth-metal atoms (M) with halogenated molecules, which are of interest because of the large number of reactive channels that can be open.[1−13]

Although many efforts were made in the past to understand the reactions of M with halogen molecules (X_2) and a very good model to describe these reactions was developed,[9,13] it seems interesting to study the reactions of M with diatomic interhalogens (XY). These systems double the number of exit channels and bring in the question of chemical branching, where two different product molecules are formed in several electronic states. In this respect Kowalski et al. have studied the chemiluminescence of various reactions of M with XY and pointed out important details of the dynamics.[10,14,15]

Reactions of M with fully halogenated methanes containing different halogens, $CX_{4-n}Y_n$, were the subject of many studies in the past using a variety of experimental methods such as the measurement of products angular distributions for Ba + CF_3I,[16] LIF studies of Ba + CF_3I,[17,18] Sr* and Sr, Ba* and Ba + CF_3Cl, CF_3Br and $CFCl_3$,[19] Ca, and Sr + CF_3Br and CF_3I,[20] spin−orbit state dependence for Ca(^3P_J) + halogenated compounds,[8] orbital alignment of Ca($^1P_1$) + HCl, Cl_2, and CCl_4,[21] etc. Most of these studies were devoted to obtain information on the energy partitioning or electronic branching ratio of the main product.

Kowalski and co-workers[12] have also studied the reaction of Ca(^3P_J, $^1D_2$) with $CX_{4-n}Y_n$ (X, Y = F, Cl, Br), and they have reported the value of both the electronic and the chemical branching ratio. They observed the formation of CaCl(A,B) and CaBr(A,B) for all the reactions in which Cl and/or Br atoms were present in the target molecule. However, they did not observe the analogous emission from CaF (A,B) as a product when other heavier halogens were present in the target molecule, despite the available energy was high enough. These experiments were performed at moderate collision energies (20 kJ/mol).

Since it has been suggested that there should be a lack of chemical specificity when translational energies are high compared to the bond strengths,[22,23] so that all of the possible products should be observed, we present here the results of our studies on the reactions of Ca(^3P_J) with CF_2Cl_2 and $CF_2{=}CCl_2$ at high collision energies (220 kJ/mol) in order to determine the possibility of generation of CaF(A,B) as a reaction product, as well as to characterize the chemiluminescence and the chemical and electronic branching ratio of the products.

In this work, we found a strong dependence of the chemical branching ratio CaCl/CaF on the specific target molecule. The differences observed for both reaction are rationalized in terms of the harpoon model and the characteristics of the molecular orbital (MO) of the target molecule in which the electron enters, as previously suggested by different authors.[24−26]

2. Experimental Section

All the experiments were carried out under beam-gas configuration and single collision conditions. A schematic view of

* Corresponding author. E-mail: jferrero@mail.fcq.unc.edu.ar. Fax: +54-351-4334188.

10.1021/jp026928q CCC: $25.00
Published on Web 08/12/2003

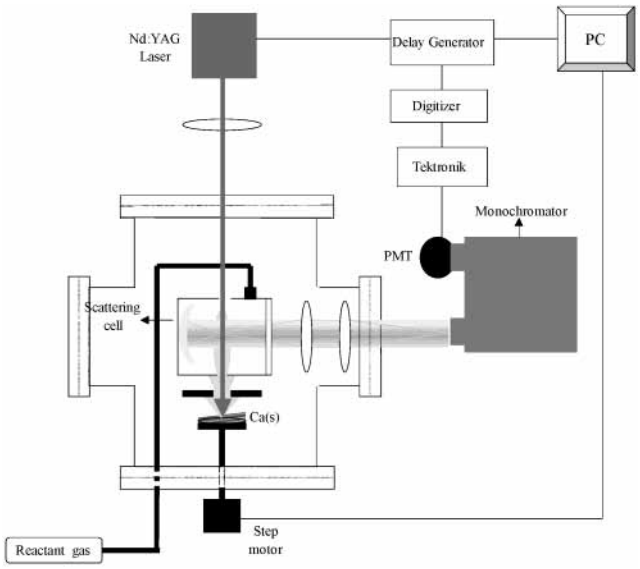

Figure 1. Schematic view (not to scale) of the experimental setup.

the experimental apparatus is shown in Figure 1. The main chamber consists of a stainless steel central cylinder with a quartz window in the front, to allow the entrance of the ablation laser beam and a BK7 glass window perpendicular to the central axis in order to detect the fluorescence. The chamber was evacuated with a Varian 1200 l/s vacuum diffusion pump system which provided a background pressure lower than 10^{-6} Torr.

The scattering reaction cell was placed into the main chamber and consisted of a cubic metal cell 6 cm long with two coaxial orifices of 0.5 cm diameter.

The excited-state calcium ($Ca(^3P)$) beam was generated by free laser ablation of a rotating solid Ca sample (Alfa AESAR, purity > 99%) using the focused pulsed radiation from the first harmonic (1064 nm) of a Nd:YAG laser (Laseroptics, LND 532) that passed through both orifices in the scattering cell. The laser was operated at 10 Hz and the beam was focused with a lens (EDS, BK7, $f = 40$ cm) onto the Ca sample. The output energy of the laser was 8.0 mJ. Under these conditions, the incident fluence was 4.0 J/cm^2. This procedure generated a pulsed atomic beam of short temporal duration (8 μs fwhm). To characterize the Ca beam, a set of experiments was performed to measure the total ablated mass of Ca using a quadrupole mass spectrometer with a channeltron detector (Balzers QMS 200). A more complete analysis of the Ca beam is given in section 4.a.

The Ca beam passed through a 0.5 cm diameter collimator into the scattering cell containing the reactant gas. The reactants (CF_2Cl_2, PCR Research Chemicals, Inc., purity >99%, and $CF_2{=}CCl_2$ PCR, Research Chemicals, Inc., purity >97%) were degassed by several freeze and pump cycles and used without further purification. The pressure in the scattering cell was kept lower than 0.8 mTorr to ensure single collision conditions while the pressure in the main chamber was always lower than 1×10^{-5} Torr. Since CaCl (A,B) and CaF (A,B) excited states are short-lived (18−38 ns),[27] the single collision condition is also ensured even at the higher pressures used.

The chemiluminescence was collected perpendicularly to the beam axis by an optical system that focused the reaction volume onto the entrance slit of a 30 cm focal length monochromator (McPherson) provided with a 1200 L/mm grating. The output of the monochromator was coupled to a photomultiplier (Hamamatsu R636) polarized at 1300 V. The width of the entrance and exit slits of the monochromator were 250 μm. Under these conditions, the spectral resolution was 0.3 nm.

The signals were digitized by a DSA 524 (Thurbly-Thandar) digital storage adapter; five signals were averaged for each spectral point and subsequently integrated using a PC.

3. Energetics

Figure 2 shows the energy levels for the systems studied in this work. The zero in the energy scale was taken as the sum of the heats of formation of $Ca(^1S)$ and the target molecules. The heats of formation used in this work were as follows: $\Delta H_f(CF_2Cl_2) = -492 \pm 5$ kJ/mol,[28] $\Delta H_f(CF_2Cl) = -279 \pm 8$ kJ/mol,[29] $\Delta H_f(CFCl_2) = -96 \pm 4$ kJ/mol,[29] $\Delta H_f(CF_2{=}CCl_2) = -328 \pm 10$ kJ/mol,[30] $\Delta H_f(CF_2{=}CCl) = -76 \pm 10$ kJ/mol,[30] $\Delta H_f(CF{=}CCl_2) = 88 \pm 10$ kJ/mol,[31] $\Delta H_f(CaF) = -272.0$ kJ/mol,[32] and $\Delta H_f(CaCl) = -104.6$ kJ/mol.[32] The energy of the molecular terms of CaF and CaCl and the atomic terms were taken from refs 33−35 and 28, respectively. The average collision energy was determined as described in section 4.b, and it was assumed that the internal energy of the reactants was negligible compared with the broadness of the collision energy distribution.

4. Results

(a) Characterization of the Ca(^{3}P) Beam. Characterization of the ablated atomic Ca beam was necessary in order to determine the reactive electronic state of the beam and the collision energy of the reactions.

The emission spectrum of the ablated Ca beam was recorded at different distances from the ablation point. When the spectrum was obtained at 0.1−0.2 cm from the target, the emissions from a number of atomic and ionic species were observed, indicating that ions and excited atoms were present in the microplasma formed at this short distance, as expected.

The emission intensity of a given transition ($I[i]$) can be related to the number density of the excited electronic state ($N[i]$) as follows:[8]

$$N[i] = \frac{I[i]}{A_{(i\rightarrow j)} f_i} \qquad (1)$$

where f_i is the degeneracy of the i electronic state and $A(i \rightarrow j)$ is the transition probability from the i to the j electronic state. Using eq 1 and the intensities of the $Ca(^1P \rightarrow {}^1S)$ (422.7 nm) and $Ca^+(^2P \rightarrow {}^2S)$ (396.8 nm) transitions, the $N[Ca(^1P)]/N[Ca^+(^2P)]$ number density ratio was determined to be approximately 1/100. Under these conditions, the relative concentration of $Ca(^3P)$ as measured from the transition $Ca(^3P \rightarrow {}^1S)$ (657.5 nm) was negligible.

As the separation of the observation point from the Ca surface increased, the spectrum changed, showing a decrease in the concentration of ions and an increase in the concentration of $Ca(^3P)$. Regarding the ions, the emission from the various states observed near the surface completely disappeared at that distance. Thus, when the spectrum was recorded at 5.0 cm from the ablation point the ratio $N[Ca(^1P)]/N[Ca^+(^2P)]$ was 1 and the number density of $Ca(^3P)$ was at least 4000 times larger than that of $Ca^+(^2P)$. In addition, when the Ca beam was analyzed at 12 cm from the ablation point using the mass detector with the ionization source turned off, the measured electron current was zero, indicating that ions were not present in the beam, at that distance.

The presence of clusters in laser ablation experiments is well documented.[36] Specifically, the spectroscopy and electronic structure of Ca_2 has been studied, using laser ablation and beam

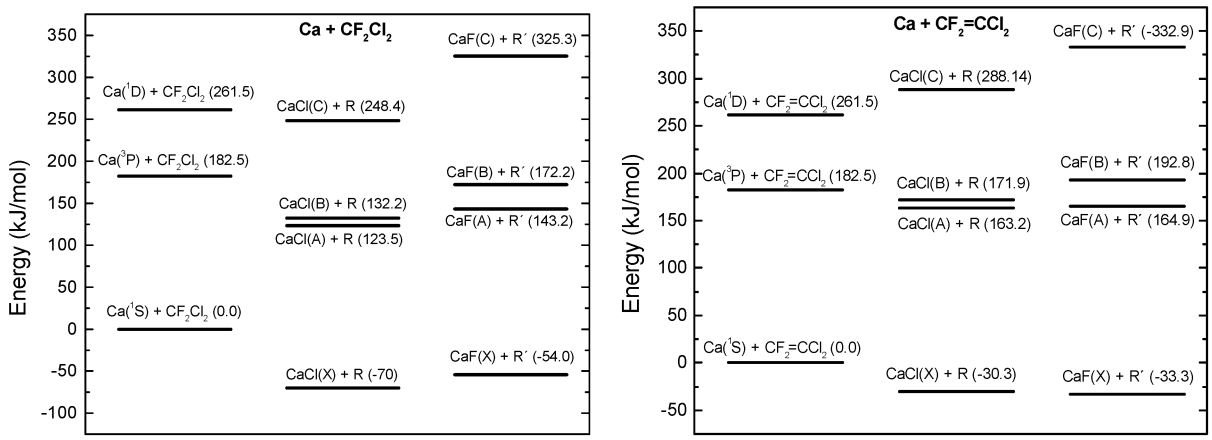

Figure 2. Electronic energy levels of reactants and products for the reactions of $Ca(^3P)$ with CF_2Cl_2 (left) and $CF_2{=}CCl_2$ (right), calculated as mentioned in section 3. R stands for CF_2Cl or $CF_2{=}CCl$ and R′ stands for $CFCl_2$ or $CF{=}CCl_2$. Numbers in parenthesis correspond to energy values in kJ/mol. The average translational energy is not included.

techniques,[36] at high stagnation pressures (2−3 atm) so that extensive adiabatic cooling took place. At lower pressures, only atomic transitions were observed. From these data, we assume that the presence of clusters should not be relevant under our experimental conditions.

To determine whether $Ca(^3P)$ or $Ca(^1S)$ is the reactive species responsible for the chemiluminescence, the $N[Ca(^3P)]/N[Ca(^1S)]$ ratio was decreased by placing Cu grids in front of the atomic beam in order to quench the $Ca(^3P)$ state. This procedure also resulted in an attenuation of the total number density of atoms in the beam in the range 40−70%, depending on the grid used. The integrated intensity of the emission due to $Ca(^3P)$ was measured together with the integrated emission from CaCl(A), CaCl(B), and CaF(A). Simultaneously, the total mass of the attenuated beam was also determined using the quadrupole mass detector. These results showed that the concentration of $Ca(^3P)$ decreased more than the total Ca so that when the beam was attenuated 70%, the intensity due to $Ca(^3P)$ was reduced to 90%. This was the highest attenuation we could use in order to obtain a good signal-to-noise ratio. The signals were then converted to relative values dividing each intensity by that obtained without the grid. In every case, plots of the intensity of the emissions of the diatomic products against those corresponding to $Ca(^3P)$ were linear with an average intercept of -0.02 ± 0.05 and a slope of 0.996 ± 0.092, as obtained by a linear regression analysis.

Considering these observations, we conclude that at distances larger than 5.0 cm from the ablation point the concentration of ions and highly excited atoms in the beam was negligible compared with that of the $Ca(^3P)$ state, and therefore, the contribution of those species, as well as $Ca(^1S)$ to the observed chemiluminescence spectra can be neglected. Consequently, in this study, we used a Ca beam flight distance of 5.5 cm from the ablation point to record the chemiluminescence from the reaction products, so that we can safely assign the chemiluminescence of all the products, CaCl(A), CaCl(B), and CaF(A), for both reactants, to reaction with $Ca(^3P)$.

(b) $Ca(^3P)$ Velocity Distribution and Relative Collision Energy. It is well established that free laser ablation produces species with high translational energies and broad multimodal distributions.[37−40]

The TOF of the excited atoms was recorded by observing the $^3P_1 \rightarrow {}^1S_0$ transition at 657.5 nm through a narrow band interference filter (EDS, $d = 24.15$ mm, cwl = 656 nm and fwhm = 10 nm). The nominal flight distance, L, from the solid target to the detection region was 5.5 cm. The time-resolved

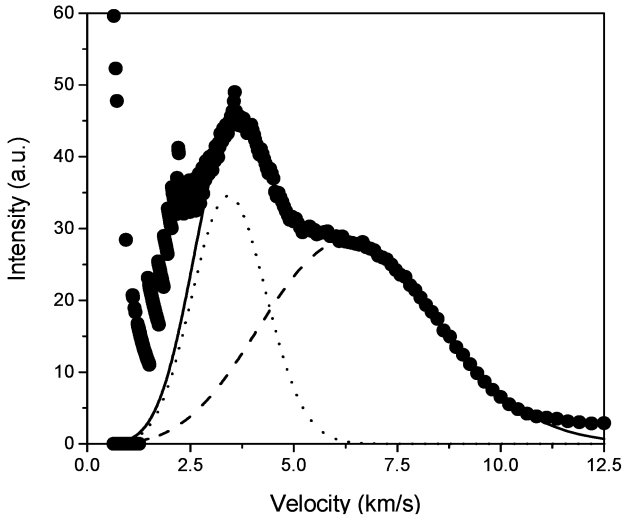

Figure 3. Estimated velocity distribution for the Ca atom beam from TOF of the emission corresponding to the $^3P_1 \rightarrow {}^1S_0$ transition: (●) experimental distribution; (···) coldest component; (- -) hottest component; (—) total fitting.

signal was corrected by the metaestable radiative decay of $Ca(^3P_1)$ ($A = 2460\ s^{-1}$)[28] and converted from number density $N_{den}(t)$ to flux distribution $N_{flux}(t)$.

The velocity distribution, $f(v)$, was obtained by directly inverting the corrected experimental TOF distribution, $N_{flux}(t)$, taking into account the time → velocity Jacobian transformation factor $dv = -L/t^2\ dt$. The final transformation equation is $f(v) \propto t^2(N_{flux}(t))/L$.

The experimental distribution was fitted to a shifted Maxwell−Boltzmann distribution that goes smoothly from the Maxwellian form of an effusive beam to the commonly used representation for the velocity distribution of a supersonic beam:[41,42]

$$f(v) = Av^3 \exp[-(v - v_0)^2/\sigma_b^2] \qquad (2)$$

Here A is the normalization factor, v_0 is the stream velocity and $\sigma_b = [2kT/m]^{1/2}$ is the width of the velocity distribution. Also, T stands for the translational temperature, k is the Boltzmann constant, and m is the atomic mass of Ca.

The experimental velocity distribution clearly presents two components[43] (Figure 3), so that the fit to the experimental results using eq 2 required the addition of two of those terms, each one with a different temperature. This behavior and the broadness of the distribution are typical of beams produced by

TABLE 1: Parameters that Characterize the Two Components of the Velocity Distribution of Ca(^3P_J) and the Collisional Energy for Both Systems

	$Ca(^3P_J) + CF_2Cl_2$		$Ca(^3P_J) + CF_2{=}CCl_2$	
	coldest	hottest	coldest	hottest
A	$(1.27 \pm 0.04) \times 10^{-9}$	$(2.5 \pm 0.2) \times 10^{-10}$	$(1.27 \pm 0.04) \times 10^{-9}$	$(2.5 \pm 0.2) \times 10^{-10}$
v_0 (km/s)	2.54 ± 0.04	3.0 ± 0.2	2.54 ± 0.04	3.0 ± 0.2
T (K)	4800 ± 200	33000 ± 1000	4800 ± 200	33000 ± 1000
v_{mp} (km/s)	3.4	6.3	3.4	6.3
$\langle E_k \rangle$ (kJ/mol)	60	412	60	412
$\langle E_k^i \rangle_t$ (kJ/mol)	46	310	47	317
relative contribution (%)	34	66	34	66
$\langle E_k^i \rangle_t$ (kJ/mol)	220		225	

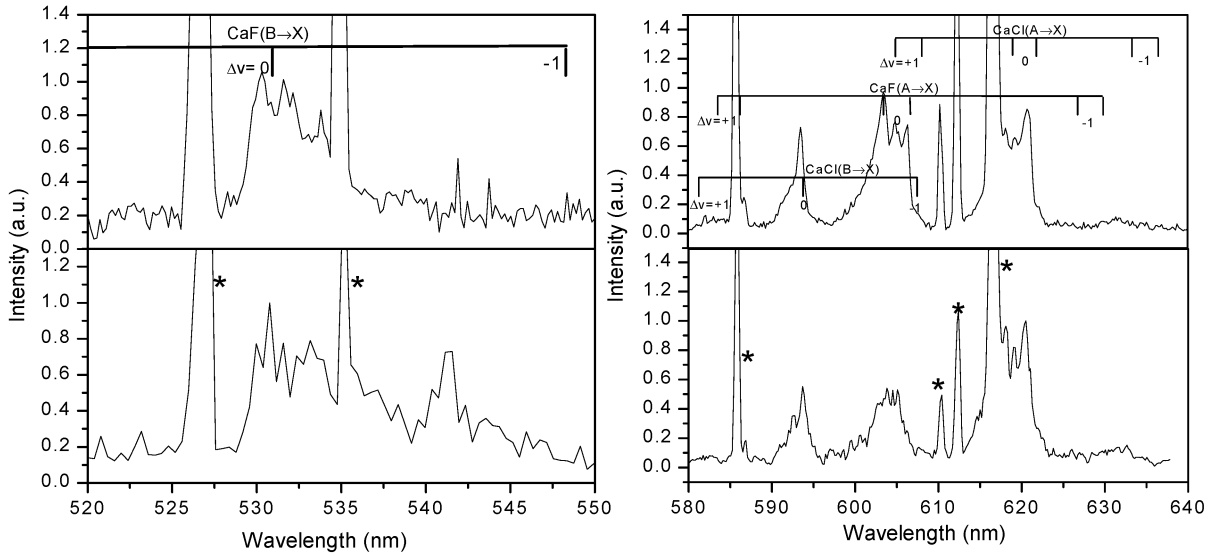

Figure 4. Spectra of the chemiluminescence observed in the reaction of ablated Ca(^3P_J) atoms with 0.48 mTorr of CF_2Cl_2 (lower panel) and 0.45 mTorr of $CF_2{=}CCl_2$ (upper panel). The left panel shows the (B → X) transition for CaF and the right panel shows the (A → X) transitions for CaF and CaCl and the (B → X) transition for CaCl. All the spectra are normalized to the maximum of the chemiluminescence. The lines marked with stars correspond to allowed atomic transitions coming from the plasma glow in the ablation zone.

laser ablation.[44,45] In the present case, in addition to the two main components considerable structure is apparent at low kinetic energies. This structure corresponds to data collected at the end of the ablation process, when the emission signal is weak and noise becomes progressively more important, affecting the quality of the measurements. Therefore, although the presence of an early structure cannot be ruled out, it could also be an experimental artifact produced during inversion of data collected at long times after the laser pulse, and consequently, it was not considered.

The parameters obtained from the best fit are shown in Table 1, as well as the most probable velocity (v_{mp}) and the mean kinetic energy $\langle E_k \rangle$, calculated as $\langle E_k \rangle = 3kT/2$.

The mean kinetic energy of each component of the atomic beam could subsequently be used to calculate the relative collision energy $\langle E_k^i \rangle$ of the reagent pair, considering the thermal motion of the target gas. Estler and Zare have estimated $\langle E_k^i \rangle$ using the following expression:[42]

$$\langle E_k^i \rangle = \frac{3}{2} k T_{\text{eff}} \tag{3}$$

where T_{eff} is a mass weighted effective temperature given by

$$T_{\text{eff}} = \frac{T_{\text{Ca}} m_i + T_i m_{\text{Ca}}}{m_{\text{Ca}} + m_i} \tag{4}$$

In the above equation, T_{Ca} is the translational temperature of a particular component of the Ca beam, m_{Ca} is the atomic mass of Ca; m_i stands for the mass of CF_2Cl_2 or $CF_2{=}CCl_2$ and T_i, which was taken as the room temperature (298 K), is the temperature of the polyatomic reactant. The values obtained for $\langle E_k^i \rangle$ are shown in Table 1.

(c) Chemiluminescent Spectrum. Figure 4 shows the chemiluminescent spectra for the reactions of Ca(^3P) with CF_2Cl_2 and $CF_2{=}CCl_2$ in the ranges 520−550 and 580−635 nm. Several emissions from different electronic excited states of CaCl and CaF were observed. Our spectra were taken under relatively low resolution (0.3 nm) so that only the $\Delta v = 0, +1, -1$ vibrational sequence of the $A(^2\Pi_\Omega) \rightarrow X(^2\Sigma^+)$ and $B(^2\Sigma^+) \rightarrow X(^2\Sigma^+)$ band systems for CaCl and CaF were identified.[33−35] The emission due to the $C(^2\Pi_\Omega) \rightarrow X(^2\Sigma^+)$ transition from CaCl or CaF could not be observed in any of the spectra.[34,35]

The chemiluminescence spectra in Figure 4 are quite similar in the region of CaCl($A(^2\Pi_\Omega)$ and $B(^2\Sigma^+) \rightarrow X(^2\Sigma^+)$) transitions but differ in the region of the CaF($A(^2\Pi_\Omega) \rightarrow X(^2\Sigma^+)$) transition, suggesting that the product internal excitation of CaF(A) is different for both reactions. This result is in good agreement with our previous work in which a very high rotational excitation in CaF(A) was found for the reaction of Ca* with CF_2Cl_2.[43] In that particular case a transition from Hund's coupling case a to case b is induced by collision energy, so that a change in the spectral shape is observed.

The spectra were recorded at different reactant pressures and all the emission bands were integrated. Plots of integrated emission intensities vs reactant pressure yielded straight lines (Figure 5) from whose slopes (α) (Table 2) the chemilumines-

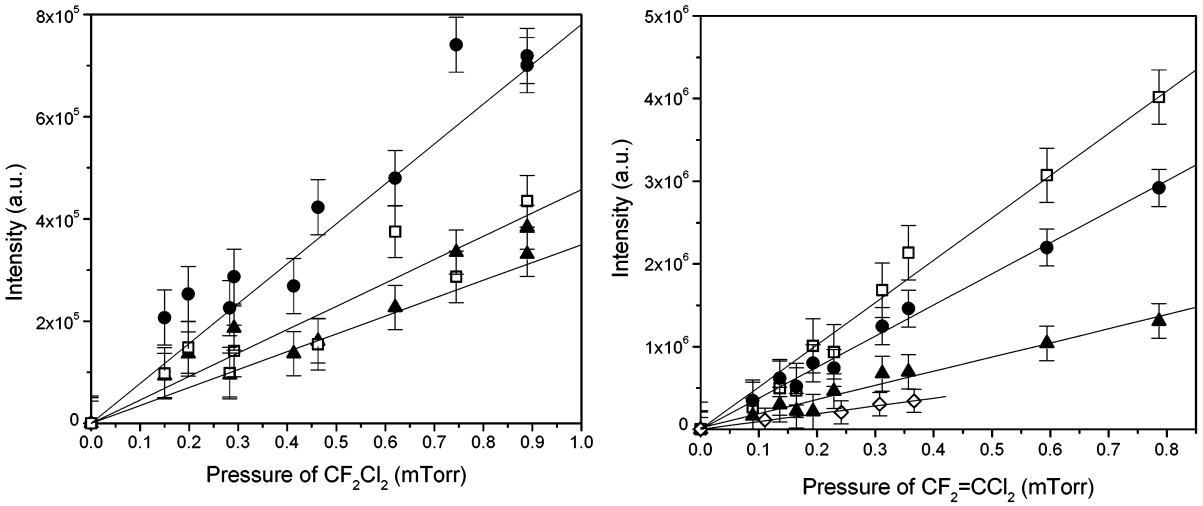

Figure 5. Integrated emission intensity of several product electronic states at different reactant pressures, for the reactions of Ca(^{3}P) with CF_2Cl_2 (left) and CF_2═CCl_2 (right): (□) CaF(A); (◇) CaF(B); (●) CaCl(A); (▲) CaCl(B).

TABLE 2: Slope Values (α) That Characterize the Pressure Dependence of the Integrated Emission Intensity of Several Product Electronic States (Figure 5) and Electronic ($\Gamma_{A/B}$) and Chemical ($\Gamma_{(CaF^*/CaCl^*)}$) Branching Ratios

	slope [(au/Torr)/10^8]			
reactants and products	$\alpha_{CaX(A)}$	$\alpha_{CaX(B)}$	$\Gamma_{A/B}$	$\Gamma_{CaF^*/CaCl^*}$
Ca* + CF_2Cl_2 → CF_2Cl + CaCl*	8.6 ± 0.4	3.8 ± 0.2	2.3 ± 0.2	0.5 ± 0.1
$CFCl_2$ + CaF*	5.0 ± 0.6	1.6 ± 0.6[a]	3 ± 1	
Ca* + CF_2═CCl_2 → CF_2═CCl + CaCl*	38 ± 1	18 ± 1	2.1 ± 0.2	1.1 ± 0.1
CF═CCl_2 + CaF*	50 ± 2	10 ± 4	5 ± 2	

[a] This value was estimated only from two spectra, since the signal/noise ratio was very low.

cent cross sections (σ_{chem}) were extracted, using the following expression[4]

$$I_{chem} = \frac{(I(^3P_1))_0\langle v\rangle}{A_{(^3P_1\rightarrow{}^1S)}f_{J=1}}\sigma_{chem}n_g = \alpha n_g \qquad (5)$$

where I_{chem} is the integrated chemiluminiscence of a given emission band; $(I(^3P_1))_0$ is the atomic emission intensity of Ca(^{3}P$_1$) when the target gas is not present and $A(^3P_1 \rightarrow {}^1S)$ is the spontaneous emission coefficient, for the Ca(^{3}P$_1$) → Ca(^{1}S) transition; $f_{J=1}$ stands for the fraction of Ca(^{3}P) in the $J = 1$ level, $\langle v\rangle$ is the mean relative collision velocity, and n_g is the reagent gas density.

Since the velocity distribution is broad and the value of $f_{J=1}$ is unknown, it was not possible to extract reliable values for σ_{chem} for each electronic state of the products. However, we should note that the composition and velocity of the Ca beam is determined by the ablation process, so that if the ablation conditions and the flight distance are kept constant for all the experiments, the slope ratios (α_i) (Table 2) should depend only on the relative chemiluminescent cross sections for two different reactive channels. In this way, we obtained estimates for the electronic branching ratios, $\sigma_A/\sigma_B = \Gamma_{A/B}$, for production of CaCl and CaF in A and B states (Table 2). Table 2 also shows the values for the chemical branching ratio $\Gamma_{(CaF^*/CaCl^*)}$ for the excited (A + B) states, estimated as follows:

$$\Gamma_{(CaF^*/CaCl^*)} = \frac{\sigma_{CaF(A)} + \sigma_{CaF(B)}}{\sigma_{CaCl(A)} + \sigma_{CaCl(B)}} = \frac{\alpha_{CaF(A)} + \alpha_{CaF(B)}}{\alpha_{CaCl(A)} + \alpha_{CaCl(B)}} \qquad (6)$$

In this case the value of the chemical branching ratio depends strongly on the target molecule, indicating different dynamics for each reaction.

Also, we obtained the ratio for the total chemiluminesce cross-section for the halogenated methane and olefin, considering the electronic excited states (A and B) for CaF and CaCl, as follows:[12]

$$\left(\frac{\sigma_{CF_2=CCl_2}}{\sigma_{CF_2Cl_2}}\right)_{chem} = \frac{[\sum_i \sigma_i]_{CF_2=CCl_2}}{[\sum_i \sigma_i]_{CF_2Cl_2}} \cong \frac{[\sum_i \alpha_i]_{CF_2=CCl_2}}{[\sum_i \alpha_i]_{CF_2Cl_2}} = 6 \pm 1 \qquad (7)$$

where the subscript *i* stands for the CaCl(A), CaCl(B), CaF(A), and CaF(B) for each reaction.

This value will be recalled in the next section to compare the dynamics of both reactions.

5. Discussion

There is ample evidence that the reaction of Ca(^{3}P) with halogenated molecules take place through an electron jump process.[2,5,8,12,21,24−26] Consequently, this mechanism will provide the basis for the analysis of the reactions reported in this work.

Even though the determination of the value of the total reaction cross-section was not feasible from our experiments, we can compare the chemiluminescent cross-sections for the reaction of Ca(^{3}P) with both reactants. The chemiluminescent cross-section for the reaction with CF_2═CCl_2 was 6 times larger than the corresponding value for the reaction with CF_2Cl_2, indicating that the distance at which the reaction occurs is larger for the former compound. This result is in good agreement with those reported by Teule at al.[26] for the reactions of Sr(^{3}P) with saturated and unsaturated hidrofluorocarbons. They reported that the LIF signal intensities of the SrF($X^2\Sigma$) for the reactions of

$Sr(^3P)$ with $CHF{=}CH_2$, $CF_2{=}CH_2$ $CHF{=}CHF$ and C_6H_5F were 1 order of magnitude stronger than those for the reactions with CH_3F, C_2H_5F, and $C_2H_4F_2$.[26]

An appropriated theoretical framework, as a first approach, to get information about the reaction mechanisms from the chemical and electronic branching ratios is given by the information theory, which compares the experimental values ($\Gamma_{(CaF^*/CaCl^*)}$ and $\Gamma_{A/B}$) with the prior statistical results ($\Gamma^0_{(CaF^*/CaCl^*)}$ and $\Gamma^0_{A/B}$) for several models, assuming the participation of different degrees of freedom of the reactants in the reaction.[46] The fraction of trajectories x_i, which results in the production of the ith electronic state, was calculated from the following expression:[47]

$$x_i \propto \frac{g_i}{(\omega_e B_e)_i}(E_T - E_i)^\beta \tag{8}$$

g_i is the electronic degeneracy (2 for A states and 1 for B states) of the electronic state at energy E_i; $(w_eB_e)_i$ are the vibrational and rotational spectroscopic constants, extracted from refs 34 and 35 for CaCl and refs 33 and 35 for CaF; E_T stands for the total energy available to the products, which was calculated as the electronic energy of the Ca atom and the relative collision energy (Table 1), and β is a factor that accounts for the degrees of freedom involved in the reaction.

Then for the chemical branching ratio, $\Gamma^0_{(CaF^*/CaCl^*)}$, we obtain

$$\Gamma^0_{(CaF^*/CaCl)} = \frac{\left[\sum_i \frac{g_i(E_T - E_i)^\beta}{(\omega_e B_e)_i}\right]_{CaF}}{\left[\sum_j \frac{g_j(E_T - E_j)^\beta}{(\omega_e B_e)_j}\right]_{CaCl}} \tag{9}$$

while the electronic branching ratio, $\Gamma^0_{A/B}$, is given by

$$\Gamma^0_{A/B} = \frac{g_A(\bar{\omega}_e B_e)_B}{g_b(\bar{\omega}_e B_e)_A}\frac{(E_T - E_A)^\beta}{(E_T - E_B)^\beta} \tag{10}$$

Figure 6 shows the values of $\Gamma^0_{(CaF^*/CaCl^*)}$ and $\Gamma^0_{A/B}$ calculated from eqs 9 and 10, for values of β from 2.5 to 10.5 and 2.5 to 13.5 for CF_2Cl_2 and $CF_2{=}CCl_2$, respectively:

(I) For $\beta = 2.5$ (rigid rotor harmonic oscillator (RRHO) approximation) the dark product (CF_2Cl or $CFCl_2$ and $CF_2{=}CCl$ or $CF{=}CCl_2$) is considered as an atom, without internal excitation.[46]

(II) For $\beta = 10.5$ (Ca + CF_2Cl_2) or $\beta = 13.5$ (Ca + $CF_2{=}CCl_2$), where $\beta = 3N - 7.5$,[48] the energy is supposed to be distributed in all the available vibrational and rotational modes of the dark product (N atoms nonlinear full complex estimation).[46,48]

Figure 6a shows that the theoretical calculations ($\Gamma^0_{(CaF^*/CaCl^*)}$) produce much lower values than the experimental results of 0.5 and 1.1 for CF_2Cl_2 and $CF_2{=}CCl_2$ respectively (Table 2). However, the theoretical results are in agreement with those reported by Kowalski and co-workers[12] for the reaction of Ca* with several polyhalogenated methanes, who concluded that the low values of $\Gamma^0_{(CaF^*/CaCl^*)}$ and the absence of CaF* chemiluminescence could be due to a statistical distribution of the energy.

The disagreement with the statistical prediction indicates that dynamical factors are important in these reactions, under the experimental conditions of our work. Also, the difference in the chemical branching ratios for both reactions indicates a relatively higher production of CaF(A+B) for the reaction of $Ca(^3P)$ with the olefin than with the methane (Table 2), which suggested that different mechanisms are taking place for each reaction.

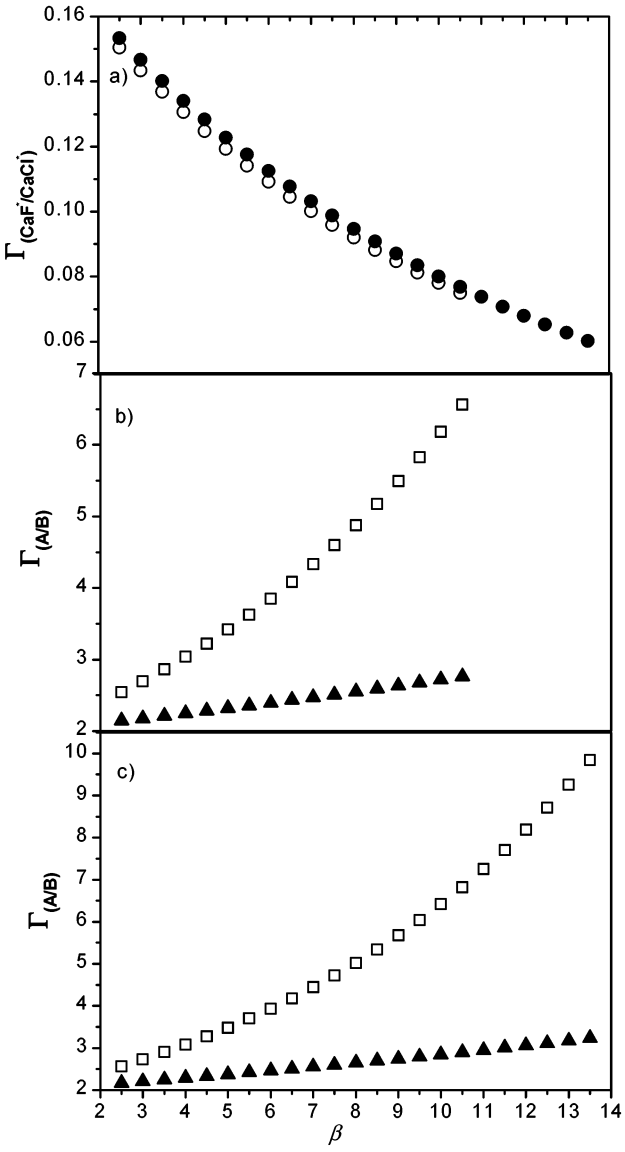

Figure 6. Calculated chemical ($\Gamma^0_{(CaF^*/CaCl^*)}$) and electronic ($\Gamma^0_{A/B}$) branching ratio as a function of β: (a) $\Gamma^0_{(CaF^*/CaCl^*)}$ for the reactions of $Ca(^3P)$ with (○) CF_2Cl_2 and with (●) $CF_2{=}CCl_2$; (b) $\Gamma^0_{A/B}$ for (▲) CaCl and (□) CaF obtained from the reaction of $Ca(^3P)$ with CF_2Cl_2; (c) $\Gamma^0_{A/B}$ for (▲) CaCl and (□) CaF obtained from the reaction of $Ca(^3P)$ with $CF_2{=}CCl_2$.

Following similar arguments than in previous works[24−26,48,49] the present results can be rationalized in terms of the MO theory and the harpoon mechanism, where as a first step in the reaction, the electron is supposed to jump from $Ca(^3P)$ to the lowest unoccupied molecular orbital (LUMO) of the reactant molecule. Therefore, the broad variety of dynamical processes found in the reactions of alkaline-earth-metal atoms with halogen-containing molecules could be explained in terms of the characteristics of the LUMO and the electronic structure of the molecular anion formed as a consequence of the electron jump.

For the sake of clarity, in the following sections we will discuss both reactions separately.

$Ca(^3P) + CF_2Cl_2$ Reaction. Several authors have performed experiments on dissociative electron attachment (DEA) to CF_2Cl_2.[50,51] From these measurements they observed the presence of a low energy resonance at 0.71 eV, corresponding to the production of Cl^-, and a higher energy resonance at 3.55 eV associated with the formation of F^-.

MO calculations show that the low energy resonance can be described as a process in which the extra electron occupies a MO with σ^*(C−Cl) character in the ground-state configuration of the molecular anion.[51,52] The higher energy resonance can be ascribed to a situation in which the incoming electron occupies a MO with appreciable σ^*(C−F) character, which thus corresponds to an excited electronic state of the molecular anion.[51] These MOs are strongly antibonding and the anion undergoes very fast dissociation to $CF_2Cl + Cl^-$ or $CFCl_2 + F^-$.

Therefore, the reactive electron affinities (REAs)[53] associated with σ^*(C−Cl) and σ^* (C−F) are $REA_{\sigma^*_{C-Cl}} = -0.71$ eV and $REA_{\sigma^*_{C-F}} = -3.55$ eV, respectively.[50,51]

Aflatooni and Burrow[50] also measured the vertical attachment energies (VAEs) of CF_2Cl_2 for formation of the lower temporary anions by electron transmission spectroscopy (ETS). The VAE associated with the temporary occupation of the σ^*(C−Cl) MO is 0.97 eV and that associated with the occupation of the σ^*(C−F) MO is 3.86 eV.[50] The VAEs correspond to the energy required to attach an electron into the MOs at the equilibrium geometries of the neutral molecules and they are related to the vertical electron affinities (VEAs) by VAE = −VEA.[54]

The REAs are lower than the VEA because the cross-section for DEA (σ_{DEA}) is the product of the attachment cross-section (σ_0) and the survival probability (P) which expresses the probability that the ionic system will survive dissociation with respect to electron loss, $\sigma_{DEA} = \sigma_0 P$.[51]

Since the REAs values are associated with the maximum for the production of Cl^- and F^-, in the following discussion, we prefer the use of REAs instead of VEAs; however, the final conclusions do not change.

As a consequence of the existence of two values of REAs there are also two different crossing radii (R_c) on the potential energy surface for the reaction of Ca* with CF_2Cl_2, given by: $R_c(Å) = 14.4/(IE_{Ca(^3p)} - REA_{\sigma^*_{C-X}})$,[55] where $IE_{Ca(^3P)} = 4.1$ eV is the ionization energy of $Ca(^3P)$ taken from ref 28. The outer radius ($R_o = 2.99$ Å) is associated with the electron jumping to the ground electronic state of the molecular anion (σ^*(C−Cl)) since it has a larger reactive electron affinity (− 0.71 eV), and the inner radius ($R_i = 1.88$ Å) corresponds to the electron jumping to the excited electronic state of the molecular anion (σ^*(C−F)) with a lower reactive electron affinity (−3.55 eV).

If the electron jump always occurs at R_o, the electron enters into the strongly antibonding σ^*(C−Cl) MO and the molecule should undergo very fast dissociation into CF_2Cl and Cl^-, which will combine with Ca^+ to produce CaCl. Then, the dissociation to $CFCl_2$ and F^- would not take place and CaF will not be observed.

In line with this argument, Kowalski and co-workers[12] did not observe CaF in the reaction of Ca* with polyhalogenated methanes at low collision energies (20 kJ/mol), indicating that the electron jump at R_i was very unlikely under those conditions.

The electron jump does not necessarily occur with unit probability at R_o, permitting the system to access to R_i. As the collision velocity increases, the diabatic transitions at R_o become less probable[49] and R_i can be reached. Consequently, the excited ionic state can be populated to undergo very fast decay into CF_2Cl and F^-, so that CaF can be formed.

The chemical branching ratio can be calculated using the electron jump model as follows:[55]

$$\Gamma_{(CaF^*/CaCl^*)} = \frac{(IE_{Ca(^3P)} - REA\text{-}Cl_{\sigma_C^*})^2}{(IE_{Ca(^3P)} - REA_{\sigma C-Cl^*})^2} = 0.4 \quad (11)$$

This value is in close agreement with the experimental value of 0.5 ± 0.1 found in the present work.

Following ref 20, we compared the equilibrium distance (R_e) of CaCl (A,B) (2.42 Å)[34] and CaF(A,B) (1.95 Å)[28,33] with the corresponding crossing radii, 2.99 and 1.88 Å, respectively. For this reaction, the calculated crossing radii are comparable with the equilibrium distance for the diatomic products, indicating that the electron jump takes place at a distance near R_e. In fact, the chemical branching ratio evaluated using R_e is 0.65, in close agreement with the experimental value (0.5) and with the value estimated from the crossing radii (0.4).

The large amount of energy released allows population of both the $A^2\Pi$ and $B^2\Sigma^+$ states of CaCl and CaF. Comparison of the electronic branching ratios, $\Gamma_{A/B}$, 2.3 for CaCl and 3.0 for CaF (Table 2), with the theoretical values presented in Figure 6b shows that the experimental values lie closer to the RRHO case than to the full-complex approximation, in good agreement with the model proposed above, in which the electron enters into σ^* orbitals and the molecular anion undergoes very fast dissociation.

$Ca(^3P) + CF_2{=}CCl_2$ Reaction. Burrow et al.[56] examined the formation of temporary negative ion in $CF_2{=}CCl_2$ by ETS. In those measurements, they found that the total scattering cross section presents several peaks as the electron energy increases. From the analysis of the experimental results, they ascribed the lowest energy peak to the temporary occupation of the lowest π^* MO, with a resulting anion of $^2\Pi$ symmetry that corresponds to the LUMO. This interpretation was supported by ab initio self-consistent field calculations.[56]

Illenberger et al.[57] employed electron-attachment spectroscopy to study the formation and dissociation of negative ions formed by attachment of low energy (0−15 eV) electrons to $CF_2{=}CCl_2$. From these measurements, they observed the formation of a long-lived parent negative ion ($CF_2{=}CCl_2^-$), with a resonance at 0 eV electron energy, which can be associated with the entrance of the electron into the LUMO. Since in their experimental setup the time-of-flight of the ions from the source to the detector was larger than 10 μs, the autodetachment and dissociative lifetime must be of the same order of magnitude to allow the observation of the parent ion. Also, these authors detected the formation of Cl^- and F^-, with a narrow resonance peak around 1 eV for the former and a broad band centered at 6−7 eV for the latter, that were associated with the reactive electron attachment to the σ^* MOs with C−Cl and C−F character, respectively. In addition, other reactive ionic channels were observed but they are not considered here since they are not relevant for the reaction of $Ca(^3P)$ with $CF_2{=}CCl_2$.

The chemical branching ratio for the reaction of $Ca(^3P) + CF_2{=}CCl_2$, can be calculated from eq 11, assuming that it occurs through the same mechanism as for CF_2Cl_2, with a crossing radius of 2.82 Å associated with the formation of Cl^- and 1.36 Å for the production of F^-. Then, the calculated value for the chemical branching ratio is 0.23. This value is far from the experimental result (1.1 ± 0.1), indicating that a mechanism in which the electron enters in strongly antibonding σ^* MOs associated with the C−Cl and C−F bonds is very unlikely for this reaction. In addition, if the electron jump takes place close

to the equilibrium distance of the diatomic product, as in the case of CF_2Cl_2, then both reactions should have similar chemiluminescent cross sections, in disagreement with the experimental value of $6 + 1$.

The above conclusion is not surprising, since the electron is transferred to the LUMO, which in this case is a π^* orbital with a slightly nonbonding or antibonding character in the C−Cl or C−F bonds.[26,58] In this process a long-lived molecular anion $CF_2{=}CCl_2^-$ with $^2\Pi$ symmetry is generated.[56,57] Dissociation from this state would result in $CF_2{=}CCl^-$ and Cl,[56,58,59] so that, to allow for the release of Cl^- and F^-, it should be necessary a transfer of the electron to the C−Cl and C−F σ^* MOs, corresponding to strongly repulsive $^2\Sigma$ states.[26,56,58]

There are theoretical evidences that the ethylene and fluoroethylene $^2\Pi$ anions are unstable with respect to out-of-plane distortion;[60] the same behavior was observed in chloroethylenes.[56] A similar distortion was probed to be likely in the case of $CF_2{=}CCl_2$[57] where such motion would permit the anion to cross over several intersecting dissociative $^2\Sigma$ surfaces. This mechanism could therefore allow temporary anions initially formed in a $^2\Pi$ state to dissociate along repulsive $^2\Sigma$ surfaces associated with the dissociation to $Cl^- + CF_2{=}CCl$ and $F^- + CF{=}CCl_2$. The Cl^- and F^- anions generated in this process can then be attracted by Ca^+ to form CaCl and CaF.

In the harpoon model the reactive cross-section is assumed to depend on the crossing radius at which the electron jumps.[55] For the reaction of Ca* with $CF_2{=}CCl_2$, the radius is unique since it corresponds to the electron jump into the π^* MO. Then, CaCl and CaF should be formed with the same cross-section, yielding $\Gamma_{(CaF^*/CaCl^*)} = 1$ in good agreement with the experimental value (1.1 ± 0.1).

Again, as in the case of the reaction with CF_2Cl_2, the energy released is large enough as to allow population of the excited electronic states of both products, CaCl and CaF. In this case, the measured electronic branching ratios $\Gamma_{A/B}$ were 2.1 and 5.0 for CaCl and CaF, respectively (Table 2). Inspection of Figure 6c shows that the experimental branching for CaF presents a large departure from the calculated value with the RRHO approximation and it is closer to that obtained using $\beta = 7.5$ ($\Gamma^0_{A/B} = 4.7$). Also the experimental $\Gamma_{A/B}$ for CaCl is in good agreement with the calculated for $\beta = 7.5$ ($\Gamma^0_{A/B} = 2.6$).

Since the best agreement with the experimental values is obtained for $\beta = 7.5$, the internal modes should be participating to some extent, implying that a collision complex is produced, in agreement with the formation of a long-lived $^2\Pi$ anion after the electron jump. Verdasco et al.,[6] suggested a similar interpretation for the reaction $Ca(^3P) + SF_6$. In this case instead of an intermediate complex, $M^+\cdots SF_6^-$, that does not dissociate immediately after the electron jump, they suggested a statistical-dynamical mechanism involving a $Ca^+\cdots F\cdots SF_5^-$ intermediate with the electronic energy in the Ca−F bond determined by dynamics and statistical behavior of the other internal degrees of freedom.

In line with the above arguments, we consider that, for the case of the olefin, the electron enters into the π^* orbital with an associated EA (0 eV) that corresponds to the resonance at 0 eV found by Illenberger et al.[56] The calculated crossing radius is 3.51 Å, leading to a cross section of 38.7 Å^2, which is therefore the value for the chemiluminescent cross sections for the reactive channels yielding CaCl* and CaF*. For the methane the chemiluminescent cross-section for the production of CaCl* is 28.1 Å^2 and for the production of CaF* is 11.1 Å^2. Then we obtain

$$\left(\frac{\sigma_{CF_2=CCl_2}}{\sigma_{CF_2Cl_2}}\right) = \frac{[\sigma_{CaCl} + \sigma_{CaF}]_{CF_2=CCl_2}}{[\sigma_{CaCl} + \sigma_{CaF}]_{CF_2Cl_2}} \cong 2 \qquad (12)$$

Although this value is in agreement with the higher reactivity of $CF_2{=}CCl_2$ compared to CF_2Cl_2, it is too small compared with the experimental result. Therefore, either the crossing radius for the olefin is larger than 3.51 Å, as calculated above or the actual EA of $CF_2{=}CCl_2$ for the entrance of the electron into the π^* orbital is larger than 0 eV. The EA of $CF_2{=}CCl_2$ can be estimated replacing $\sigma_i = \pi[14.4/(IE_{Ca(^3P)} - EA_i)]^2$ in eq 12 and equating to the experimental value of the relative chemiluminescent cross-section (6 ± 1). Then, using IE = 4.1 eV,[28] $EA_{\sigma^*C-Cl} = REA_{\sigma^*C-Cl} = -0.71$ eV,[52] and $EA_{\sigma^*C-F} = REA_{\sigma^*C-F} = -3.55$ eV[52] for CF_2Cl_2, the result is $EA_{CF_2=CCl_2} = 1.75$ eV.

This value indicates that the neutral molecule is stabilized by the entrance of an electron, in good agreement with others halogenated ethenes, i.e., C_2Cl_3H and C_2Cl_4 whose adiabatic EAs where found to be 0.4[61] and 0.64 eV,[61,62] respectively.

Note that in the case of the reaction of CF_2Cl_2 with $Ca(^3P)$ the dynamics is dominated by the entrance of the electron into different σ^* orbitals and the subsequent fast formation of the Cl^- or F^- anions; as a consequence, the reactive cross sections depend on the REAs for those orbitals. On the other hand, the dynamics for the reaction of $Ca(^3P)$with $CF_2{=}CCl_2$ is determined by the entrance of the electron into a π^* orbital and the consequent formation of a $CF_2{=}CCl_2^-$ stable anion, so that, the important quantity for the estimation of the reactive cross-section is the adiabatic EA, since this is the property that measured the relative stability of the anion compared to the neutral molecule.

6. Conclusions

The most important results of the present investigations are as follows.

(1) The chemiluminescent cross-section for the reaction of $Ca(^3P)$ with $CF_2{=}CCl_2$ is larger than the corresponding value for the reaction with CF_2Cl_2.

(2) The CaF(A,B) product was observed for both reactions at variance with the results informed by Kowalski et al.[12] for reactions of $Ca(^3P,^1D)$ with polyhalogenated methanes at lower collision energy (20 kJ/mol) than in the present work (220 kJ/mol).

(3) The chemical branching ratio $\Gamma_{(CaF^*/CaCl^*)}$ strongly depends on the target molecule, suggesting the presence of different reaction mechanisms for each molecule.

(4) The electronic branching ratios $\Gamma_{A/B}$ for CaCl are very similar for both reactions but they are different for CaF, indicating different dynamical behavior for each reaction.

In summary, significant differences are observed in the reaction of hyperthermal $Ca(^3P) + CF_2Cl_2$ with respect to $Ca(^3P) + CF_2{=}CCl_2$. These differences can be satisfactorily explained in terms of the harpoon mechanism and the MO theory as due to the characteristics of the LUMO of each molecule and the stability of the molecular anion formed after the electron jump. Comparison of the experimental results with prior estimations shows that the reaction with CF_2Cl_2 is direct as expected by the entrance of the electron into fast decaying σ^* orbitals, associated with different crossing radii. The reaction with $CF_2{=}CCl_2$ occurs through the formation of a collision complex with the partial participation of the internal degrees of freedom, in agreement with the formation of a temporary anion that results

from the entrance of the electron into a π^* orbital that dissociates after coupling with dissociative ionic surfaces.

Even though a tentative explanation to the higher reactivity of the olefin relative to the methane was provided in this work, more experimental and theoretical studies, specially related to the energetic and geometry of the neutral and anionic states of this reactants, are clearly necessary to fully understand this difference, which has been unclear until now.

Acknowledgment. This work has been supported by CONICET, CONICOR, Fundación Antorchas, SeCyT (UNC), ANPCyT, and SeCyT−ECOS.

References and Notes

(1) Kierzkowski, P.; Lawruszczuk, R.; Kowalski, A. *Chem. Phys. Lett.* **1994**, *225*, 369.
(2) Orea, J. M.; Laplaza, A.; Rinaldi, C. A.; Tardajos, G.; González, Ureña, A. *Chem. Phys.* **1997**, *220*, 337.
(3) Garay, M.; Rinaldi, C. A.; Orea, J. M.; González Ureña, A. *Chem. Phys.* **1998**, *236*, 343.
(4) Garay, M.; Esteban, M.; Verdasco, E.; Gonzáles Ureña, A. *Chem. Phys.* **1995**, *195*, 235.
(5) Garay, M.; Orea, J. M.; González Ureña, A. *Chem. Phys.* **1996**, *207*, 451.
(6) Verdasco, E.; Sáez Rábanos, V.; Aoiz, F. J.; González Ureña, A. *J. Phys. Chem.* **1987**, *91*, 2073.
(7) Engelke, F.; Sander, R. K.; Zare, R. N. *J. Chem. Phys.* **1976**, *65*, 1146.
(8) Furio, N.; Campbell, M. L.; Dagdidian, P. J. *J. Chem. Phys.* **1986**, *84*, 4332.
(9) Kowalski, A.; Menzinger, M. *J. Phys. Chem.* **1990**, *94*, 1899.
(10) Kierzkowski, P.; Pranszke, B.; Kowalski, A. *Chem. Phys. Lett.* **1996**, *254*, 391.
(11) Pranszke, B.; Kierzkowski, P.; Kowalski, A. *Chem. Phys. Lett.* **1999**, *309*, 183.
(12) Pranszke, B.; Kierzkowski, P.; Kowalski, A. *Chem. Phys. Lett.* **2000**, *317*, 220.
(13) Kierzkowski, P.; Kowalski, A.; Wren, D.; Menzinger, M. *J. Phys. Chem. A.* **2000**, *104*, 8346.
(14) Kierzkowski, P.; Pranszke, B.; Wolinski, P.; Kowalski, A. *Chem. Phys. Lett.* **1996**, *251*, 323.
(15) Kierzkowski, P.; Pranszke, B.; Kowalski, A.; Menzinger, M. *Z. Naturforsch.* **2000**, *55a*, 433.
(16) Lin, S.-M.; Mims, C. A.; Herm, R. R. *J. Phys. Chem.* **1973**, *77*, 569.
(17) Smith, G. P.; Whitehead, J. C.; Zare, R. N. *J. Chem. Phys.* **1977**, *67*, 4912.
(18) Johnson, M. A.; Allison, J.; Zare, R. N. *J. Chem. Phys.* **1986**, *85*, 5723.
(19) Solarz, R. W.; Johnson, S. A. *J. Chem. Phys.* **1979**, *70*, 3592.
(20) Keijzer, F.; Teule, J. M.; Bulthuis, J.; de Graaff, G. J.; Hilgeman, M. H.; Janssen, M. H. M.; van Kleef, E. H.; van Leuken, J. J.; Stolte, S. *Chem. Phys.* **1995**, *207*, 511.
(21) Rettner, Ch. T.; Zare, R. N. *J. Chem. Phys.* **1982**, *77*, 2416.
(22) Rothe, E. W.; Tang, S. Y.; Reck, G. P. *Chem. Phys. Lett.* **1974**, *26*, 434.
(23) Tang, S. Y.; Mathur, B. P.; Rothe, E. W.; Reck, G. *J. Chem. Phys.* **1976**, *64*, 1270.
(24) Han, K.; He, G.; Lou, N. *Chem. Phys. Lett.* **1993**, *203*, 509.
(25) Brenner, D. M.; Smith, G. P.; Zare, R. N. *J. Am. Chem. Soc.* **1976**, *98*, 6707.
(26) Teule, J. M.; Janssen, M. H. M.; Stolte, S.; Bulthuis, J. *J. Chem. Phys.* **2002**, *116*, 6079.
(27) Dagdigian, P. J.; Cruse, H. W.; Zare, R. N. *J. Chem. Phys.* **1974**, *60*, 2330.
(28) NIST Data Base; http://webbook.nist.gov.
(29) Ley, L.; Masanet, J.; Carlap, F.; Lesaclaux, R. *J. Phys. Chem.* **1995**, *99*, 1953.
(30) Caballero, N. B.; Castellano, E.; Cobos, C. J.; Croce, A. E.; Pino, G. A. *Chem. Phys.* **1999**, *246*, 157.
(31) Cobos, C. J. To be published.
(32) JANAF Thermochemical Tables (Third Edition). *J. Phys. Chem. Ref. Data* **1985**, *14*, Supp. 1.
(33) Kaledin, L. A.; Bloch, J. C.; McCarthy, M. C.; Field, R. W. *J. Mol. Spectrosc.* **1999**, *197*, 289.
(34) Berg, L. E.; Klynning, L.; Martín, H. *Phys. Scr.* **1980**, *21*, 173.
(35) Herzberg, G. *Molecular Spectra and Molecular Structure, Spectra of Diatomic Molecules*; Van Nostrand Reinhold: New York, 1957; Vol. I.
(36) Bodybey, V. E.; English, J. H. *Chem. Phys. Lett.* **1984**, *111*, 195.
(37) Scott, D. C.; Winterbottom, F.; Scholefield, M. R.; Goyal, S.; Reisler, H. *Chem. Phys. Lett.* **1994**, *222*, 471.
(38) Scholefield, M. R.; Goyal, S.; Choi, J.-H.; Reisler, H. *J. Phys. Chem.* **1995**, *99*, 14605.
(39) Scholefield, M. R.; Choi, J.-H.; Goyal, S.; Reisler, H. *Chem. Phys. Lett.* **1998**, *288*, 487.
(40) Krajnovich, D. J. *J. Chem. Phys.* **1995**, *102*, 726.
(41) Auerbach, J. D. In *Atomic and Molecular Beam Methods*; Scoles, G., Bassi, D., Buck, U., Lainé, D., Eds.; Oxford University Press: New York, and Oxford, England, 1988; p 362.
(42) Estler, R. C.; Zare, R. N. *Chem. Phys.* **1978**, *28*, 253.
(43) Pino, G. A.; Rinaldi, C. A.; Ferrero, J. C. *Chem. Phys. Lett.* **2001**, *349*, 463.
(44) Nakata, Y.; Okada, T.; Maeda, M. *Jpn. J. Appl. Phys.* **1995**, *34*, 4079.
(45) Eryu, O.; Murakami, K.; Masuda, K.; Shihoyama, K.; Mochizuki, T. *Jpn. J. Appl. Phys.* **1992**, *31*, 86.
(46) Bernstein, R. B.; Levine, R. D. *Adv. At. Mol. Phys.* **1975**, *11*, 215.
(47) Faist, M. B.; Levine, R. D. *Chem. Phys. Lett.* **1977**, *47*, 5.
(48) Riley, S. J.; Herschbach, D. R. *J. Chem. Phys.* **1973**, *58*, 27.
(49) Loesch, H. J.; Möler, J. *J. Chem. Phys.* **1992**, *97*, 9016.
(50) Aflatooni, K.; Burrow, P. D. *Int. J. Mass Spectrom.* **2001**, *205*, 149.
(51) Langer, J.; Matt, S.; Meinke, M.; Tegeder, P.; Stamatovic, A.; Illenberger, E. *J. Chem. Phys.* **2000**, *113*, 11063.
(52) Oster, T.; Kühn, A.; Illenberger, E. *Int. J. Mass Spectrom. Ion Processes* **1989**, *89*, 1.
(53) Chen, E. C. M.; Shuie, L−R.; D'sa, E. D.; Batten, C. F.; Wentworth, W. E. *J. Chem. Phys.* **1988**, *88*, 4711.
(54) Aflatooni, K.; Gallup, G. A.; Burrow, P. D. *J. Phys. Chem. A* **2000**, *104*, 7359.
(55) Levine, R. D.; Bernstein, R. B. In *Molecular Reaction Dynamics and Chemical Reactivity*, Oxford University Press: New York, and Oxford, England, 1987.
(56) Burrow, P. D.; Modelli, A.; Chiu, N. S.; Jordan, K. D. *Chem. Phys. Lett.* **1981**, *82*, 270.
(57) Illenberger, E.; Baumgärtel, H.; Süzer, S. *J. Electron Spectrosc. Relat. Phenom.* **1984**, *33*, 123.
(58) Clarke, D. D.; Coulson, C. A. *J. Chem. Soc. A* **1969**, 169.
(59) Wiley, J. R.; Chen, E. C. M.; Wentworth, W. E. *J. Phys. Chem.* **1993**, *97*, 1256.
(60) Paddon-Row, M. N.; Rondan, N. G.; Houk, K. N.; Jordan, K. D. *J. Am. Chem. Soc.* **1982**, *104*, 1134.
(61) Chen, E. C. M.; Wiley, J. R.; Batten, C. F.; Wentworth, W. E. *J. Phys. Chem.* **1994**, *98*, 88.
(62) Drexel, H.; Sailer, W.; Grill, V.; Scheier, P.; Illenberger, E.; Märk, T. D. *J. Chem. Phys.* **2003**, *118*, 7394.